# Finite-Element Simulation of Aluminum Temperature Field in Laser Welding

Ali MOARREFZADEH

Young  Researchers Club, Mahshahr Branch, Islamic Azad University,

Mahshahr, Iran

A_moarrefzadeh@yahoo.com
A.moarefzadeh@mahshahriau.ac.ir

Abstract: In this paper, the laser beam welding is studied and Aluminium temperature field is gained in this process. The thermal effect of laser beam that specially depends on the laser type and temperature field of it in workpiece, is the main key of analysis and optimization of this process, from which the main goal of this paper has been defined. Utilizing laser as a method to join plastic components is growing in popularity. There are two laser welding mechanisms, keyhole mode and conduction mode. Keyhole welding is widely used because it produces welds with high aspect ratios and narrow heat affected zones. However keyhole welding can be unstable, as the keyhole oscillates and closes intermittently. This intermittent closure causes porosity due to gas entrapment. Conduction welding, on the other hand, is more stable since vaporisation is minimal and hence there is no further absorption below the surface of the material. Conduction welds are usually produced using low-power focused laser beams. This results in shallow welds with a low aspect ratio. In this work, high-power $CO_2$ and YAG lasers have been used to produce laser conduction welds on 2mm and 3mm gauge AA5083 respectively by means of defocused beams. Full penetration butt-welds of  and 3mm gauge AA508 using this process have been produced. It has been observed that in this regime the penetration depth increases initially up to a maximum and then decreases with increasing spot size.

Key-Words: Aluminum, laser welding, Finite-Element, ANSYS

## 1 Introduction

Laser welding and arc welding methods have been used in many industries for a long time, and their application is being continuously developed. Laser welding has many attractive features: laser beams can be focused to a very small diameter, and can melt only very small portions of materials. For this reason, laser welding can be conducted without affecting nearby materials, thus, the heat-affected zone (HAZ) is usually very small. This makes laser welding suitable for the precise welding of small parts.

Laser beam power and profile can be adjusted or modified easily to make keyholes, thus, deep penetration welding is possible.

There are many attributes of laser light that are uniquely suited for laser welding. A beam of laser light is monochromatic (single wavelength) and collimated (parallel) and hence can be focused down to a very small spot where the photon density is high enough to melt metals and alloys in a matter of milli-seconds. Laser wavelengths are typically identified by the laser source used to produce laser light. The most commonly used for pulsed welding is 1.064 micron Nd:YAG wavelength that has the option of being transmitted through an optical fiber. A new generation of lasers called fiber lasers also have similar wavelength where the laser light is produced in the fiber itself. Fiber lasers have the benefit of producing good beam quality and hence can have much longer working distance (distance between lens and work piece), of the order of ten inches as compared to about two inches for conventional YAG lasers. Another source commercially available is the

10.64 micron CO2 laser, thought that is more often used for continuous wave welding rather than for pulsed welding.

The laser beam can travel through air or vacuum with minimal loss of energy. In some applications, the entire laser delivery hardware including focus head and fiber can be mounted inside a glove box where the environment is controlled for oxygen and water vapor contamination as is necessary for welding of Titanium. If required, the controlled environment can be produced in a more confined space with the laser energy being delivered through a quartz window.

Laser welding does not require that the part being welded be electrically conductive as is required for competing technologies including resistance welding, arc welding, and electron beam welding. Consequently, lasers have been used to weld all types of materials including metals, ceramics/glasses, and plastics. In welding of metals, all the laser energy is absorbed on the surface of the metal where as in glasses, part of the energy is absorbed on the surface while the remaining portion is absorbed in the bulk.

Welding of plastics is performed by facilitating absorption of laser energy at the weld interface either by using an absorptive layer or having one of the plastic be colored for preferential absorption.

Perhaps the most important aspect that has led to the growing use of lasers for welding is the ability to make spot welds. A laser beam focused down to a spot can heat, melt, and solidify metals in a matter of milliseconds with minimal disturbance to adjoining volume of material and components. Consequently, laser spot welding is finding ever increasing applications in all segments of manufacturing including medical devices, sensors, batteries, and microwave enclosures. Along with growth in applications, there has been substantial improvement in laser power supply capabilities including closed-loop feedback and pulse shaping. As laser pulse welding is pushed to its limits in new and unique applications, it will be increasingly important to have good understating of the laser pulse and its effect on the parts being welded. This paper presents insights into the anatomy of a laser pulse and its effect on weld size, shape, residual stress, and defects.

This fields equations are solved together. Finally by writing codes with FSI (Fluid solid Interface) and SIMPLEC way, the process is optimized. For this simulation design parameter are introduced then condition function parameters are introduced as function of design parameters. And objective function that is the temperature field of Aluminum, for achieving to the optimized fields is derived. That

has suitable condition like cooling rate, the control of expanding HAZ (Heat Affected Zone) and optimization of consumed energy, for doing the process[1].

## 2 Laser Transmission and Technical Limitations

With respect to the nature of beam delivery, there is little difference between the techniques used for metal and plastic welding. The essential difference in the plastic welding approach is the through transmission IR concept. The necessity for physical contact in the plastic welding process arises from the basic principle of laser transmission welding as shown in Fig.1. Once the parts to be joined have been brought into contact, the laser beam penetrates through the top transparent layer/component.

The beam energy is transformed into heat by the absorbent joining part, plasticizing the material at this point. The transparent part is melted by thermal conduction as a result of the physical contact with the absorbing layer. An impermeable weld is produced between the two joining partners in the weld area. Fig. 2 shows the experimental setup of the PALW system. External contact pressure is applied to achieve an uninterrupted contact between the plastic components in the weld area. Good welding quality therefore depends on the regulation of laser energy, the interaction between the laser beam and the plastic material, and good physical contact. The standard method used to create a physical contact between the two components is to incorporate a clamping system, typically utilizing pneumatic cylinders to push the parts up against a metal frame or glass plate.

Good clamping conditions can easily be achieved for smaller two-dimensional weld contours however, larger two-dimensional and three-dimensional welding contours make it difficult to maintain static contact between the joining areas along the entire welding contour[2,3].
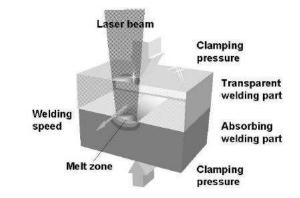
## 3 Numerical Simulation

Finite elements simulations are done in 3 steps with the main pieces:
1- Modeling by FEMB
2- The thermal study and processing
3-Post-Processing result of analysis by ANSYS software for results discussion

Modeling special techniques for a finite elements:
1-Finite elements modeling ,types and properties for model different parts.

2-The definition of material properties
3- parameter definition
4- Loading
5- Boundary and initial value definition
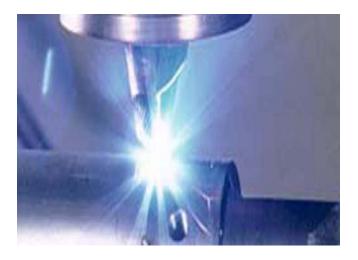6- Common interfaces definition
7- Control parameter definition



Fig.1. The laser transmission welding
principle



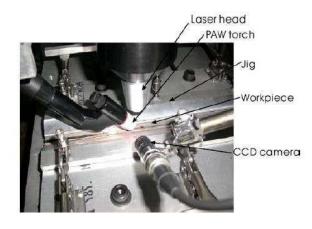Fig.2. Experimental setup of laser
system

### 3.1 Numerical solution
-In numerical method that is done with ANSYS code
the finite element (SIMPLEC) is used.
- In numerical solution by considering the interface
solid and fluid, the FSI used.

### 3.2 Finite-Element Modeling
In Fig.3, finite element model is shown. The model
is Two-dimensional and axisymmetric. In this model,
the method of meshing is manual. And the thickness
of each mesh is 0.00005 m. this meshing is done in a
way that solid and fluid mesh are exactly fixed. For
meshing of solid field (Aluminum) by considering
the study of thermal field, from the thermal elements
set, we chose the PLANE55 type. Because as
axisymmetric element with conduction property, this
element has 4 node with one degree of freedom. This
element has mesh moving property as well. for lase
field use FLUID142 element. Because this element is
so suitable for transient thermal modeling. Also this
element has thermal energy transmitting property.

### 3.3 Material Modeling
In the study that is done for solid, the isotropic
model and for fluid the ideal fluid model is used.

### 3.4 Parameter Defection
For giving data to temperature and fluid velocity,
that depend on time, the parameter is defined to the
variation of this parameters since the welding
machine is on till it is off and the workpiece cooling,
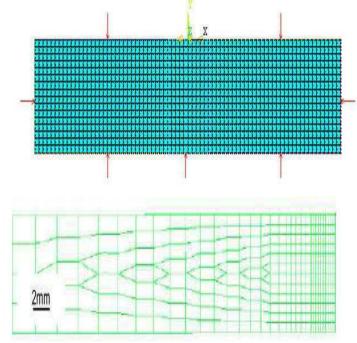is considered in the software.



Fig.4. Finite-Element Modeling

The differential Eqs. (1)–(6) are solved iteratively

by the SIMPLEC numerical procedure:

For boundary condition of fluid field:

$$\int_\Omega \partial P[\frac{1}{C^2}\ddot{P}+(\nabla)^Y \nabla P]d\Omega +$$

$$\int_{T_1} \partial P n^T \ddot{u}\, dT + \int_{T_3} \partial P \frac{1}{g}\ddot{P}\, dT = 0 \qquad (1)$$

For boundary condition of solid field:

$$\int_\Omega \partial u\,[\,P_s\,\ddot{u}+\,S^T\,DSu\,]d\Omega\,-$$

$$\int_{T_1} \partial u^T\,\bar{t}\,\,dT\,=\,0 \qquad (2)$$

Heat transfer equation
   For conduction:

$$q_X \;=\; -\,k_{xx}\,\frac{dT}{dx} \qquad (3)$$

   For convection:

$$q_h \;=\; h\,(T\,-\,T\infty\,) \qquad (4)$$

$$\frac{\partial}{\partial x}(k_{xx}\,{\partial T}/{\partial x})+Q=$$

$$\rho C\frac{\partial T}{\partial t}+\frac{hP}{A}(T-T\infty) \qquad (5)$$

Potential of heat transfer equation:

$$\Pi_p \;=\; u\,+\,\Pi_V\,+\,\Pi_q\,+\,\Pi_h$$

$$\Pi_V=-\iiint_V QTdV,$$

$$\pi_q=-\iint_{S_2} q+ds, \qquad (6)$$

$$\pi_h=\frac{1}{2}\iint_{S_1} h(T-T\infty)^2\,dS$$

### 3.5 Gas Shielding Effects

The different gas shielding configurations illustrated in Fig. 5 were used to determine top shielding effects on weld appearance. The slightly different angles were necessitated by constraints in the experimental system and fixturing limitations but do not produce significant differences in results. Beam focus was located at the workpiece surface. The different cross jet configuration affect the plasma formation over the weld. The leading edge configuration tends to blow plasma to the to-be welded location while the trailing edge and transverse direction configurations blow the plasma away from the to-be-welded location. The presence of plasma tends to absorb and defocus the beam. Unpublished tests by the authors on Aluminum parts have shown that weld penetration is decreased using the leading edge configuration. The results obtained for Aluminium using the TEM20 beam at 5.1 kW and a weld speed of 12.7 m/s also show a decreased penetration for the leading edge case. The coaxial flow configuration is not as efficient in "blowing" away the plasma as a side jet and also produced lower weld penetration.

### 3.6 Semi-quantitative analysis
It has been observed that penetration depth increases with spot radius during low-speed laser welding in the conduction mode regime. The laser beam is defocused.
Below is a 1D semi-quantitative analysis of the phenomenon. Experiments were carried out to establish the dimensions of the fusion zone in laser welding as the laser beam diameter incident on the sample was increased. The increase in the laser beam diameter was achieved by increasing the standoff distance between the lens and the work piece.

### 3.7 Location of Beam Focus
Most of the data reported here are obtained using a beam focus position at or above (~2.5mm) the workpiece surface. Martukanitz, et al. found that using beam defocusing produced better welds and avoided hole formation but beam irradiances were not measured precisely.
Park et al. located beam focus below the surface and obtained good welds. We have observed that locating the beam focus inside the weld increased the welding efficiency in that substantially higher weld speeds (16.9instead of 12.7 m/s) can be used to obtain the same penetration if the irradiance is controlled. The effect of high irradiance on weld quality will be discussed in the next section.
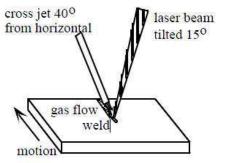
### 3.8 Weld Quality
Laser welding of Aluminium tends to produce a higher degree of spatter than for the case of Aluminium.
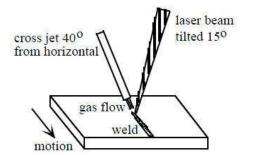A higher cross-flow was necessary to prevent spatter on the optics. High irradiances also tend to produce more spatter and lower weld surface quality for Aluminium.

The spot sizes at focus were 200 and 400 μm for the TEM00 and TEM20 beams respectively. Beam focus was located at the workpiece surface. The voids/porosities in the weld cross sections tend to be relatively small with a few larger voids. All voids were smaller than 0.1 mm.

The welds obtained with the TEM00 beam tend to have higher porosity. The irradiances used here were very similar for both beam modes. The narrower welds higher porosity could result from the smaller surface area and more constrained convection of the weld pool for expulsion of gases produced. All weld cross sections examined showed some degree of porosity regardless of edge preparation. Dry milled or wire-brushed edges had similar levels of porosity[2].
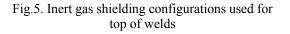
The tube seam line is slightly opened, and this gap plays a roll as a V-groove in butt welding joints, as in Fig. 6a. This V-groove enhances absorption of the laser beam by the mechanism of multiple reflections within it. To simulate this process in laboratory experiments, the jig makes two strips be positioned slightly inclined and brought into contact with each other, like conventional butt joints. The cross section of the designed jig is show in Fig. 6b, which shows two strips inclined at an angle of 5°, and the laser beam is irradiated onto the V-groove joint. Therefore, the seam welding of small-diameter pipe can be successfully simulated by butt joint welding of thin stainless steel strips.



(a) cross jet pointed at leading edge of weld pool



(b) cross jet pointed at trailing edge of weld pool

Fig.5. Inert gas shielding configurations used for top of welds



a. Tube formed prior to welding process
b. Jig used in experiments

Fig.6. Joint shape and jig system used in experiments.
a. Tube formed prior to welding process.
b. Jig used in experiments.

# 4 Welding concept for three-dimensional joining application

A new concept was recently introduced to eliminate the technical limitations encountered in the use of clamping systems and to facilitate the use of laser for three dimensional joining. With this new process the contact pressure required for the joining process is constantly regulated to act dynamically, selectively, perpendicularly and precisely at the desired joining area.

The welding concept essentially works on the contour welding principle, whereby the laser spot follows a contour and the component is sequentially welded.

A laser spot is focused on the joining plane by means of an air bearing, frictionless, rotating glass sphere as shown in Fig.7. The glass sphere lens serves as a mechanical pressing tool applied perpendicularly at each point on the joining plane. This ensures that the laser beam is only incident at the site where the contact pressure is applied.

This process concept offers the possibility of applying the necessary contact pressure concurrent with the laser beam being continuously moved along a welding contour. The air bearing glass sphere lens is fitted in a robust and compact processing head together with the optical fiber connector and other optical systems and process monitoring sensors[2].
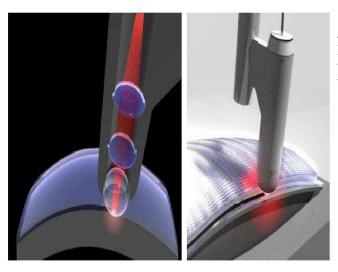
Fig.7. Schematic diagram of the
welding technique

Figures 8 and 9 show the definition of the
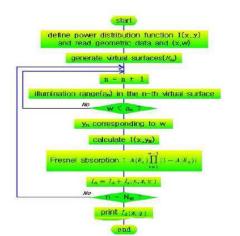intensity functions and the steps to obtain
them.



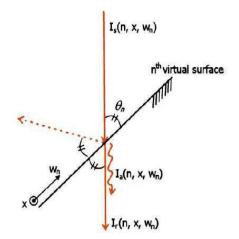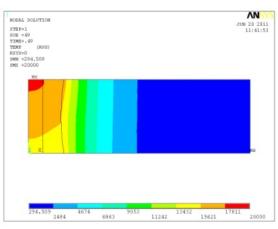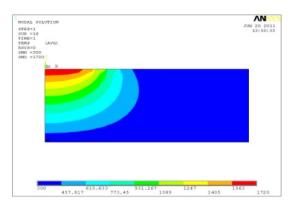Fig. 8. Steps for the calculation of intensity functions



Fig.9. Definition of the intensity functions

## 5 Result and Discussion

Fig.10. shows two-dimensional distributions of
the temperature and flow velocity in 3case
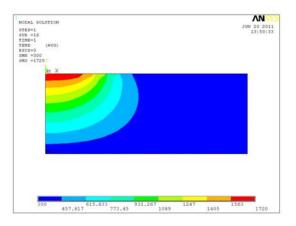thickness.







Fig.10. Two-dimensional distributions of
Aluminium temperature field and flow velocity
in (a) 4.2mm (b) 4.4mm (c) 4.6mm

Details provided in this work on Aluminium alloy
together with results obtained by other researchers
on Aluminium alloys reveal that laser beam welding

of Aluminium alloys has limitations in obtaining the desired weld strength and formability required for automotive applications. In particular, for 1.8 mm 5182 Aluminium alloy samples with shear cut edges, butt welds obtained with beams achieved ultimate tensile strength of 251 MPa, elongation of 10.4% and 75% of desired formability in terms of dome height. Martukanitz et al. results had corresponding values of 190 MPa, 5.4% and 77% respectively.

Conclusions for solid (5182 Aluminiumalloy) temperature field, completely and showing the heat transfer way between laser beam and shielding gas and between shielding gas and environment with temperature and velocities for different gases is completely shown in Fig.11.
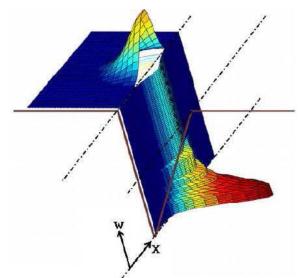


Fig.11. Solid (5182 Aluminum alloy) temperature field

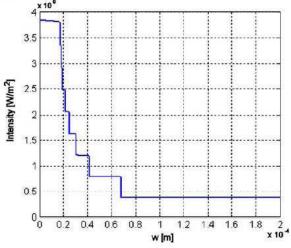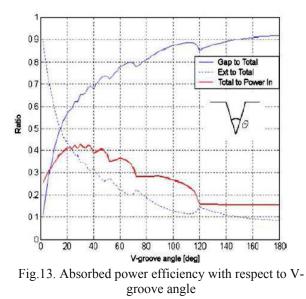Also,Fig.12. shows the final 3D distribution of absorbed intensity.



Fig.12.distribution of absorbed intensity.

The graph in Fig.13. shows some discontinuous step shapes because of the superposition effect, while the maximal intensity occurs at the bottom (w=0).
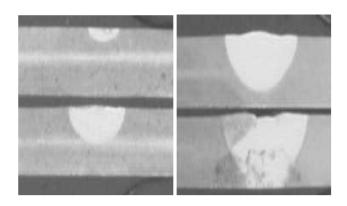
Fig.13. shows the absorbed power efficiency with respect to the groove angle. At the V-groove angle of 10°, which is the value selected in this study, the absorbed efficiency is calculated to be about 35%. The maximal efficiency can be achieved at the angle of 20°-40°. As the angle increases above this range, the efficiency is decreased to about 15%, which is almost equal to the efficiency value of the flat plate.

The multi-reflection model proposed here is valid when the V-groove wall remains at its initial geometry. But in the real situation, there occurs melting and collapse of the groove wall, which prevents the laser beam from penetrating into the bottom[8].



Fig.13. Absorbed power efficiency with respect to V-groove angle

Conduction welds were produced using high-power defocused laser beams on 2mm and 3mm gauge AA5083.

Fig.14 shows micrographs of conduction welds made from 3mm gauge AA5083. The numbering is done in order of increasing spot radius. The expected hemispherical shape characteristic of conduction welds was obtained. The variation of the penetration depth with increasing spot radius or distance from the focus becomes apparent on close examination. In all cases it was found that the aspect ratios (penetration depth divided by weld width) of the welds were less than one. Penetration depth/spot radius curves plotted showed an increase (up to a maximum) and then a decrease of penetration depth with increase in spot radius in the conduction weld regime.

This can be attributed to the interplay between decreasing power density and increasing interaction time, as the spot radius becomes larger. It is suggested that the laser beam distribution and pre-heating due to the interaction of the outer fringes of the laser beam with the work piece also contribute to this phenomenon.

Fig.15. shows micrographs of laser keyhole and conduction welds. Fig.15.a. is a micrograph of a butt weld obtained using the YAG laser at a weld in speed of 360mm/min and the work piece situated at distance of 20mm below the focus. This position produced the maximum penetration depth for the laser setup. It can be seen that the weld was a fully penetrating one. Fig.15ii is a laser keyhole weld produced by a CO2 laser at maximum power of 1750W with welding speed of 1600mm/min on 2mm AA5083. The groove on the weld surface constitutes a an area of weakness. Although the surface was wire-brushed and cleaned, a pore was clearly revealed.
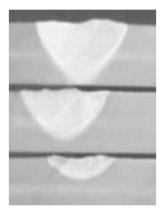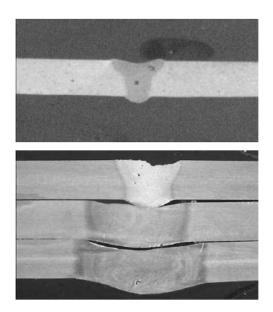


Fig.15 – (i) 3mm AA5083 LCW(YAG, Butt Weld),
v = 360mm/min,
(ii) 2mm AA5083KHW, v =1600mm/min(CO2)

# 6 Conclusion

According to result achieved from coupling field analysis and comparison of temperature field and heat transfer in laser beam welding with other process, it can be derived the laser welding have more arc length concentration of higher energy, better a stability and more welding depth to width.(specially for Aluminum tube) Laser welding is emerging as an important welding technique in plastics processing. The diverse fields of application always call for new techniques and innovative problem solving approaches.

Though various laser transmission welding techniques have been introduced that complement conventional joining methods, the innovative potential of laser transmission welding has yet to be fully exploited. By virtue of its precise and controllable application of the necessary joining force this process produces an optically perfect welding seam, which is of crucial importance in the manufacture of decorative components. A typical example is the manufacture of automobile headlights or tail lights, which require a three-dimensional welding seam.

Semi-quantitative and experimental investigations into laser conduction welding (LCW) of AA5083 using high power defocused CO2 and YAG laser beams reveal that

penetration depth increases up to a maximum and then decreases with increasing spot radius. More specifically, Semi-quantitative analysis of the LCW



Fig.14.Conduction weld for 3mm gauge AA5083 using YAG laser ;Average power = 2000W ; Weld speed = 600mm/min

process shows that the penetration depth increases with increase in spot radius when the surface temperature remains at boiling temperature. This trend is reversed when the boiling temperature is no longer sustained due to a further increase in the spot radius. This confirms that the penetration depth/spot radius variation occurs well within the conduction-welding regime, as ideally there should be no vaporization during LCW.

# Reference

[1] A. Moarrefzadeh, "Choosing suitable shielding gas for thermal optimization of GTAW process" IREME Journal, Sep 2010, pp.748-754.

[2] A. Moarrefzadeh, "Numerical simulation of temperature field by Plasma arc welding Process in stainless steel" IREMOS Journal, February 2010, pp.101-107.

[3] A. Moarrefzadeh "Numerical Analysis of α-phase Stainless Steel Thermal profile in Keyhole Plasma Arc Welding (PAW)Process" IREME Journal, Nov 2010.

[4] M. Ushio, and H. Terasaki, "plasma arc keyhole welding"Welding Journal, September 2005, pp. 331-340.

[5] Matsuda J, Utsumi A, Katsumura M, Hamasaki M, Nagata S(1988) TIG or MIG arc augmented laser welding of thick Mild steel plate. Join Mater 1(1):31–34

[6] H. Kyselica, "High–Frequency reversing arc switch for plasma welding of Aluminum" Welding Journal, May 2005, pp. 31-35.

[7] Bos,J.A., Chen,M.A, "On the Prediction of Weld Pool Size and Heat affected Zone in Shallow-Pool Welding", Transport Phenomena in Materials Processing and Manufacturing ASME, HTD Vol. 336 ,1996

[8] Williams,S.W et al "Direct Diode Laser welding of Aerospace Alloys", Laser Opto, Vol. 33, No.4, 2001

[9]Nakamura, S. et al "Detection Technique for Transition between Deep Penetration Mode and Shallow Penetration Mode in CO2 Laser Welding of Metals ", J.Phys.D:Appl. Phys. 33, pp.2941-2948

[10]Russo,A.J. et al "Two-Dimensional Modelling of Conduction- Mode Laser Welding" L.I.A. Vol 44 (ICALEO) , pp. 8-16 ,1984

[11]Paul,A. and DebRoy,T., "Free Surface Flow and Heat Transfer in Conduction Mode Laser Welding", Metallurgical Transactions B, Vol. 19B, pp. 851-858, 1988

[12]Zhao,H. and DebRoy,T., "Weld Metal Composition Change during Conduction Mode Laser Welding of Aluminium Alloy 5182", Metallurgical Transactions B, Vol. 32B, pp. 163-172, 2001

[13] Philip I Pavlik Jr., Hao Cen, Kenneth R. Koedinger, Learning Factors Transfer Analysis: Using Learning Curve Analysis to Automatically Generate Domain Models

[14] David Prata, Ryan Baker, Evandro Costa, Carolyn Rose, Yue Cui, Detecting and Understanding the Impact of Cognitive and Interpersonal Conflict in Computer Supported Collaborative Learning Environments

[15] Dovan Rai, Yue Gong, Joseph Beck, Using Dirichlet priors to improve model parameter plausibility

[16] Steven Ritter, Thomas Harris, Tristan Nixon, Daniel Dickison, R. Charles Murray, Brendon Towle, Reducing the Knowledge Tracing Space

[17] Vasile Rus, Mihai Lintean, Roger Azevedo, Automatic Detection of Student Mental Models During Prior Knowledge Activation in MetaTutor

[18] Mari‼an Simko, Maria Bielikova, Automatic Concept Relationships Discovery for an Adaptive E-course

[19] John Stamper, Ti any Barnes, An unsupervised, frequency-based metric for selecting hints in an MDP-based tutor

[20] Cesar Vialardi Sacin, Javier Bravo Agapito, Leila Shafti, Alvaro Ortigosa, Recommendation in Higher Education Using Data Mining Techniques